



## **LHCb Muon Chamber Geometry Simulation**

**S. Amato, P. Colrain**

Instituto de Física - UFRJ

**K. Harrison**

Rome I

**B. Schmidt**

CERN EP-Division

### **Abstract**

A detailed model of the LHCb muon system chambers is presented. The implementation of the model in the Geant-based simulation program SICBMC is described, and results from a test of the revised simulation are discussed.

# 1 Introduction

The description of the muon system implemented in SICBMC v234, and in earlier versions of the LHCb simulation, was very simple. Each station was represented as 2 stratified blocks, 160 mm apart. Each block consisted of a 4-mm-thick active gas gap, bounded on either side by 10 mm of honeycomb and 2 mm of aluminium. This simplified representation was used in the optimisation of the logical-channel layout [1].

Optimisation of the hardware implementation of the logical layout requires a more detailed simulation, which takes into account the materials and positions of all chambers in the muon system. In this note, we present the relevant geometrical and physical information, and describe how this information is used in SICBMC v235. Details of the layouts of physical and logical channels, and of the readout architecture, are given elsewhere [2, 3].

In Section 2 of this note we list the chamber materials used in the simulation of the Multi-Wire Proportional Chambers (MWPCs) and Resistive-Plate Chambers (RPCs) chosen for the muon system. Chamber dimensions and positions are reported in Sections 3 and 4, and the implementation in SICBMC of the revised detector description is discussed in section 5. We conclude in Section 6, showing results from checks of the new simulation.

## 2 Chamber Materials

The muon system consists of 5 stations, M1 (upstream) to M5 (downstream), each of which is divided into 4 annular regions, R1 (inner) to R4 (outer). All chambers in each region of each station are identical in terms of material composition and size. Chambers that are of the same type, but are in different regions, differ only in their x and y dimensions: their materials and thicknesses are identical. In the simulation, regions R3 and R4 of stations M4 and M5 use RPCs, each with two gas gaps; the rest of the muon system is instrumented using MWPCs, with four gas gaps each. In reality, the technology for regions R1 and R2 of station M1 is still to be decided.

### 2.1 Multi-Wire Proportional Chambers

The MWPCs of the muon system each have 4 gas gaps. A cross-sectional view of a chamber, as modelled in the simulation, is shown in Fig. 1. A single gap structure consists of 5.0 mm of sensitive gas (60% Ar, 10% CF<sub>4</sub> and 30% CO<sub>2</sub>), with 1.6 mm of G10 and 3.5 mm of honeycomb on either side. The G10 plate is sandwiched between 0.05-mm-thick layers of copper, so that the total thickness of a gap structure is 15.4 mm. Once the 4 gap structures have been assembled, a chamber is sealed by two endcaps. Each of these consists of 1.6 mm of G10 and 1 mm of aluminium. Summing up the 4 gap structures and 2 endcaps, we have a total thickness of 67.0 mm. The chambers have aluminium frames with a thickness of 1.0 mm.

### 2.2 Resistive-Plate Chambers

The RPCs used in the muon system each have 2 gas gaps, and are as shown in Fig. 2. In the simulation, a single gap structure consists of 2.0 mm of sensitive gas (96% C<sub>2</sub>H<sub>2</sub>F<sub>4</sub>, 3% C<sub>4</sub>H<sub>10</sub>, 1% SF<sub>6</sub>), sandwiched between 2.0-mm-thick phenolic plates. The two gap structures of a chamber are separated by 5.0 mm of polystyrene foam. Each endcap consists of 3.2 mm of

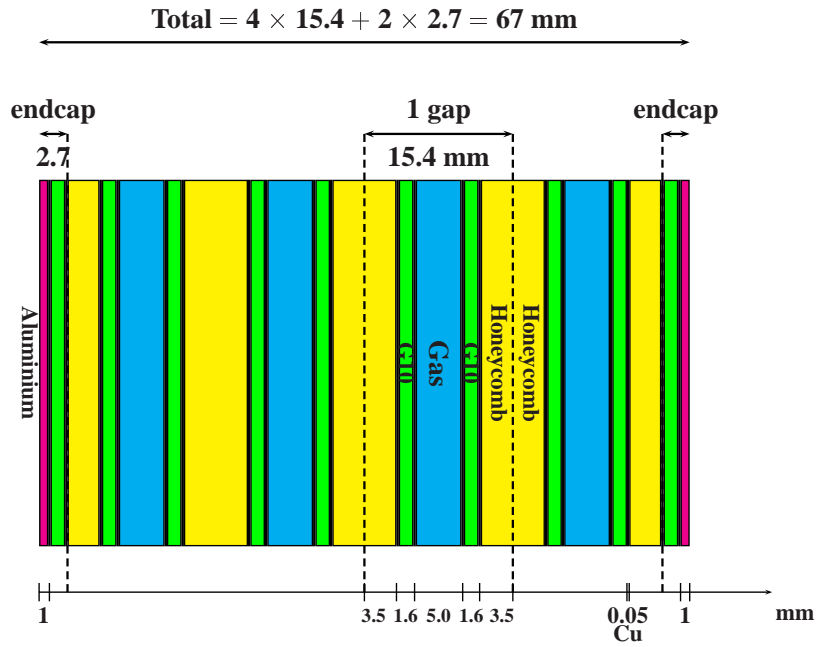


Figure 1: Material composition of the 4-gap MWPCs modelled in the simulation.

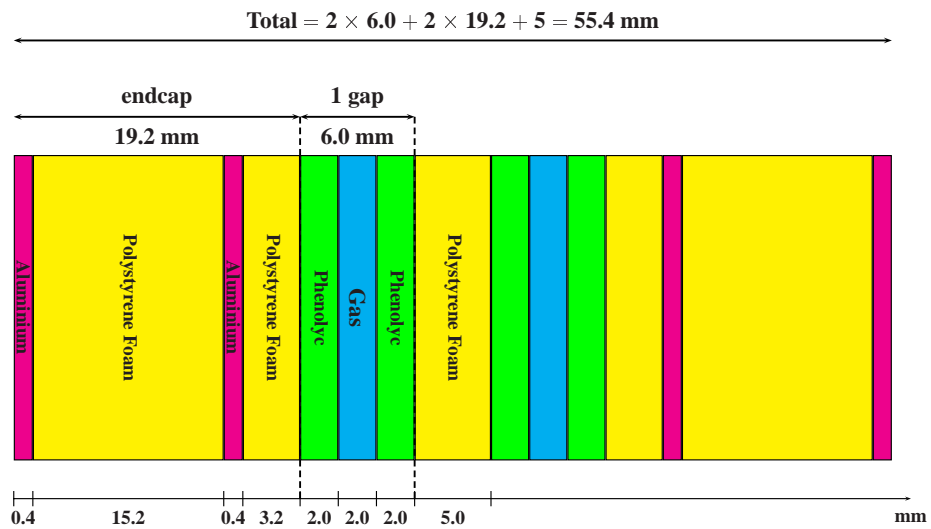


Figure 2: Material composition of the 2-gap RPCs modelled in the simulation.

polystyrene foam, 0.4 mm of aluminium, a further 15.2 mm of polystyrene foam, and 0.4 mm of aluminium. The total thickness of an RPC chamber is, then, 55.4 mm. Again, each chamber is surrounded by a 1.0-mm-thick aluminium frame.

### 3 Chamber Dimensions

For each region of station M1, Table 1 gives the x and y dimensions of the region inner bounds, and of the active gas volumes of the chambers used. It is noted that all chambers have a height of 200 mm. Chamber dimensions in x and y are 2 mm larger than the dimensions of the corresponding gas volumes, because of the aluminium frames. Dimensions of regions and chambers in stations M2 to M5 are chosen so as to be projective to M1, as seen from the interaction point.

Table 1: Dimensions in x and y of region inner bounds, and of chamber gas volumes, for each region of station M1. The M1 outer dimensions are  $3840 \times 3200 \text{ mm}^2$ .

Region	Region inner dimensions ( $\text{mm}^2$ )	Chamber gas dimensions ( $\text{mm}^2$ )
	x × y	x × y
R1	240 × 200	240 × 200
R2	480 × 400	480 × 200
R3	960 × 800	960 × 200
R4	1920 × 1600	960 × 200

### 4 Chamber Positions

The z positions for the centres of each muon station, as measured from the interaction point, are given in column 2 of Table 2. Each station will have at its centre a 50-mm-thick aluminium support structure. This support is not included in the simulation, although the space that it should occupy is reserved. The chambers of a station are arranged in 4 layers, with 2 layers (L1 and L2) in front of the support structure and 2 layers (L3 and L4) behind. The z positions of these 4 layers are shown in columns 3 to 6 of Table 2, and the layer assignments of a sub-set of chambers are shown in Fig. 3. Chambers in the same row are either all in front of the support structure or all behind. The z positions of the MWPCs (thickness of 67.0 mm) are chosen such that there is no gap in z between L1 and L2, between L2 and the support, between the support

Table 2: The z positions of the station centres, and the z offsets within a station of the 4 chamber layers.

Station	z of station centre (mm)	z of layer centre relative to station (mm)			
		L1	L2	L3	L4
M1	12105	-125.5	-58.5	+58.5	+125.5
M2	15200	-125.5	-58.5	+58.5	+125.5
M3	16400	-125.5	-58.5	+58.5	+125.5
M4	17600	-125.5	-58.5	+58.5	+125.5
M5	18800	-125.5	-58.5	+58.5	+125.5

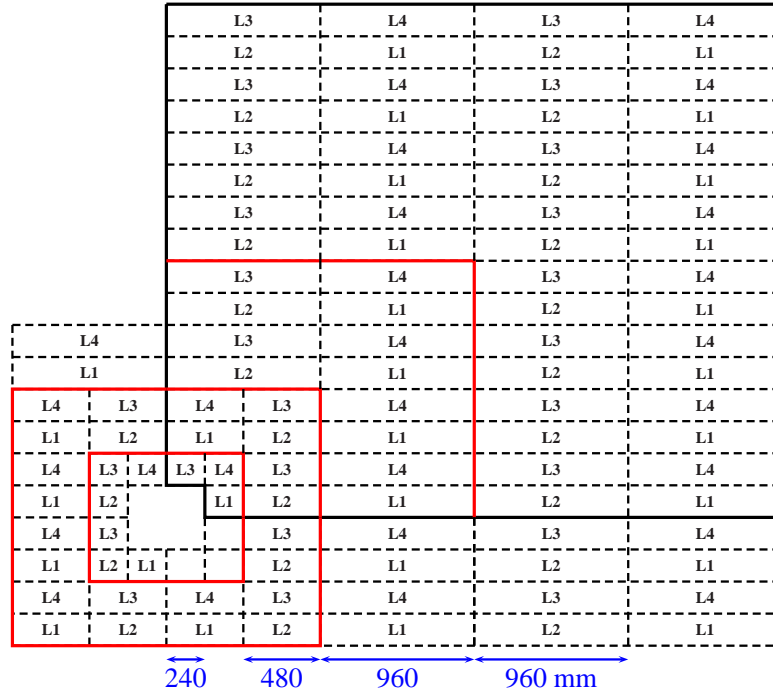


Figure 3: Arrangement of chambers as seen in x-y projection. Chambers are placed in layers, labelled L1 (upstream) to L4 (downstream), with L1 and L2 in front of the support structure, and L3 and L4 behind. The chamber x dimensions (mm) indicated are for station M1.

and L3, or between L3 and L4. The same relative positions are used for the RPCs, even though their smaller thickness (55.4 mm) would allow them to be more closely packed.

To determine the x and y coordinates of the chamber centres, we start from an ideal situation, where the chambers are placed at the z coordinate of the station centre and the gas volumes of neighbouring chambers are in direct contact (physically impossible because of the chamber frames). The centre of each chamber is then offset along the line that joins it to the interaction point, until the appropriate z coordinate (Table 2) is reached. As seen from the interaction point, this procedure results in a small overlap in y for the sensitive volumes, since the increase in angular coverage of the chambers moved towards the interaction point (L1 and L2) is greater than the decrease in angular coverage of the chambers moved away by the same distance (L3 and L4). However, given the small y dimensions of the chambers, this overlap is negligible.

Chambers adjacent in x (same row) are either all moved towards the interaction point or all moved away. Overlap in x is introduced for the chambers moved towards the interactions point, and holes in x are introduced for the chambers moved away. Overlaps and holes are minimal, since chambers adjacent in x are on the same side of the support, and have their centres separated in z by only 67.0 mm.

Figure 4 shows the y-z view of the chamber arrangement for station M1. Chambers shown in layer L1 are at a different x position from those shown in layer L2.

Figure 5 shows the arrangement of chambers in the first two rows of a quadrant, as seen in the x-z projection. Chambers in front of the support are at a different y position from those behind the support.

Table 3 shows the number of chambers per quadrant in each region of a station. The total number of chambers in the muon system is  $69 \times 4$  (quadrants)  $\times 5$  (stations) = 1380.

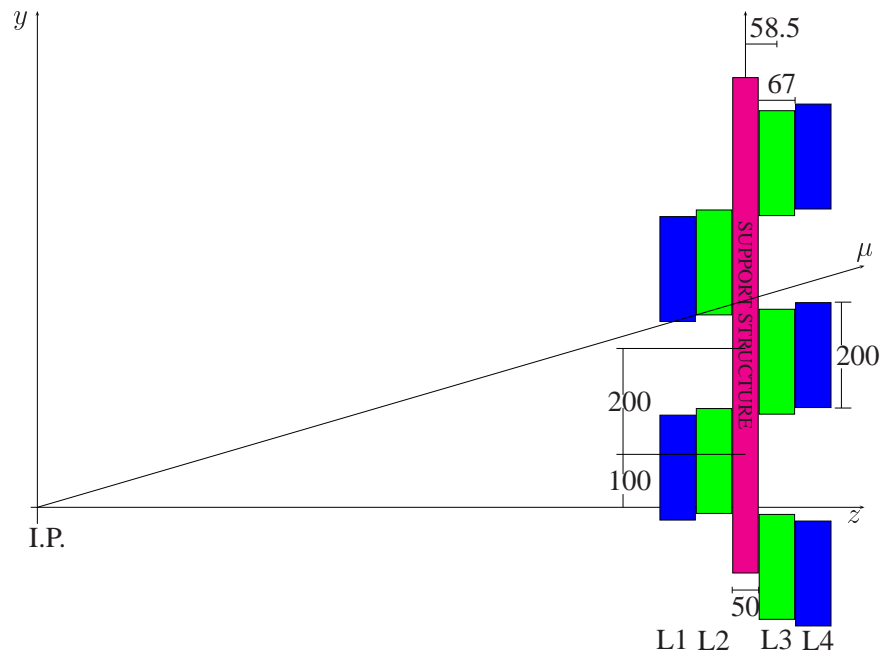


Figure 4: Arrangement of chambers as seen in  $y$ - $z$  projection. Chambers are placed in layers, labelled L1 (upstream) to L4 (downstream). Dimensions are given in mm.

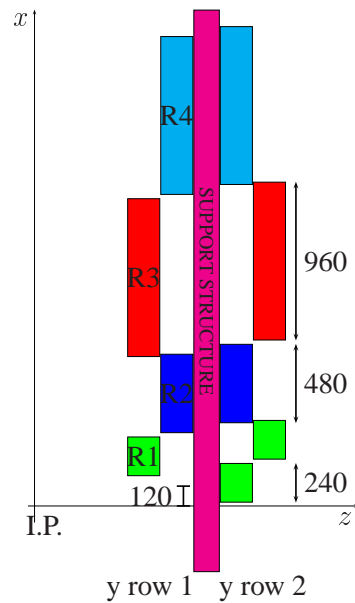


Figure 5: Arrangement of chambers in the first two rows of the upper right quadrant, as seen in  $x$ - $z$  projection. The quadrant is divided into regions, R1 to R4. Dimensions are given in mm.

Table 3: The number of chambers per quadrant in each region of a station.

Region	Chambers per quadrant
R1	3
R2	6
R3	12
R4	48
Total	69

## 5 Implementation

The information given above on chamber materials, dimensions and positions is stored in a constants-definition file for the muon system (muon.cdf) released with version v232 of the LHCb simulation database. Given the projectivity of the muon stations, and the symmetries between quadrants, the system is fully specified by giving the station  $z$  coordinates, the material thicknesses for MWPCs and RPCs, and the chamber positions and dimensions in one quadrant of station M1. In practice, a standalone program (maintained in /afs/cern.ch/user/s/sandra/public/write\_cdf) is used to expand a file containing this minimal information into the full system description stored in muon.cdf and used in SICBMC.

The code required to interpret the muon.cdf file, and to pass information to routines based on Geant 3 [4] is implemented in SICBMC v235. This code is structurally similar to the older geometry code, and provides backwards compatibility. The new code is run if the version number read from muon.cdf is 3 or higher; the old code is run for lower version numbers.

### 5.1 Structure of the cdf file

The structure of the muon.cdf file is as follows:

Number of stations

$z$  position of each station

For each station:

→ Number of regions (or chamber types)

For each region (or chamber type):

→ Number of chambers

For each chamber:

→  $z$  of centre relative to  $z$  of station;  $x$  of centre;  $y$  of centre

→ Number of gas gaps per chamber

For each gas gap:

→  $z$  of centre relative to  $z$  of chamber

→ Number of different materials in a gap structure

For each material:

→  $z$  of centre relative to  $z$  of gap;  $x$  length;  $y$  length; thickness; material

For each gas-gap frame (not considered in code):

→  $z$  relative to  $z$  of gap;  $x$  length;  $y$  length; material

→ Number of different materials in an endcap

For each material:

→  $z$  of centre relative to  $z$  of chamber;  $x$  length;  $y$  length; thickness; material

For each Chamber frame:

→  $z$  relative to  $z$  of chamber;  $x$  thickness;  $y$  thickness;  $z$  thickness; material

## 5.2 Geant hierarchy

In the simplified representation of the muon system, where a station was modelled as two stratified blocks (aluminium-honeycomb-gas-honeycomb-aluminium), each material was introduced in the Geant hierarchy as a daughterless volume, and was positioned directly in the LHCb mother volume. With the new simulation, use of this type of hierarchy would be very time consuming. To gain efficiency, we position chamber materials inside a chamber volume, then position the chamber in the LHCb mother volume. With this method, the time for initialisation and the time per event increases very little as compared with the time used previously.

## 5.3 Modified packages

The new geometry code was released with SICBMC v235 and uses dbase v232 or later. Two packages have been changed:

detdes v7:

- muginit.F - modified, calls either muginit1 or muginit2, depending on the version number in muon.cdf
- muginit1.F - new, essentially a copy of the old muginit.F, reads the old muon.cdf (version number < 3)
- muginit2.F - new, reads the new muon.cdf (version number  $\geq 3$ )
- utrect2.F - new utility routine, defines a rectangular box with a rectangular hole, centred on a given point
- mcgpar.inc - contains all of the new parameters for the geometry of the muon system (complements detdes/mugpar.inc)

simmuon v4:

- mugeom.F - modified, calls muginit.F to read muon.cdf version  $\geq 3$
- mugeom3.F - new, implements detector geometry as described in muon.cdf version  $\geq 3$ , and as unpacked by muginit2.F
- mugcham.F - new, creates a chamber volume (mother) and fills with constituent materials (daughter volumes)
- murawh - modified to call mufillrw2 for muon.cdf version  $\geq 3$
- mufillrw2 - new, fills muon raw-hits bank for muon.cdf version  $\geq 3$
- musets - modified to add an additional sensitive volume, corresponding to the RPC gas



## 6 Hit Distributions

To check that the chosen chamber layout does not introduce significant chamber overlaps or holes, and to test the implementation of the chamber geometry in SICBMC, we have examined the  $x$ ,  $y$  and  $z$  coordinates for the entry and exit points (hits) of charged tracks crossing the chamber gas volumes. The data sample considered consisted of 800 minimum-bias events (type 51), simulated using SICBMC v240r1 and dbase v233r2 (implying the baseline choice of an aluminium-beryllium beam pipe).

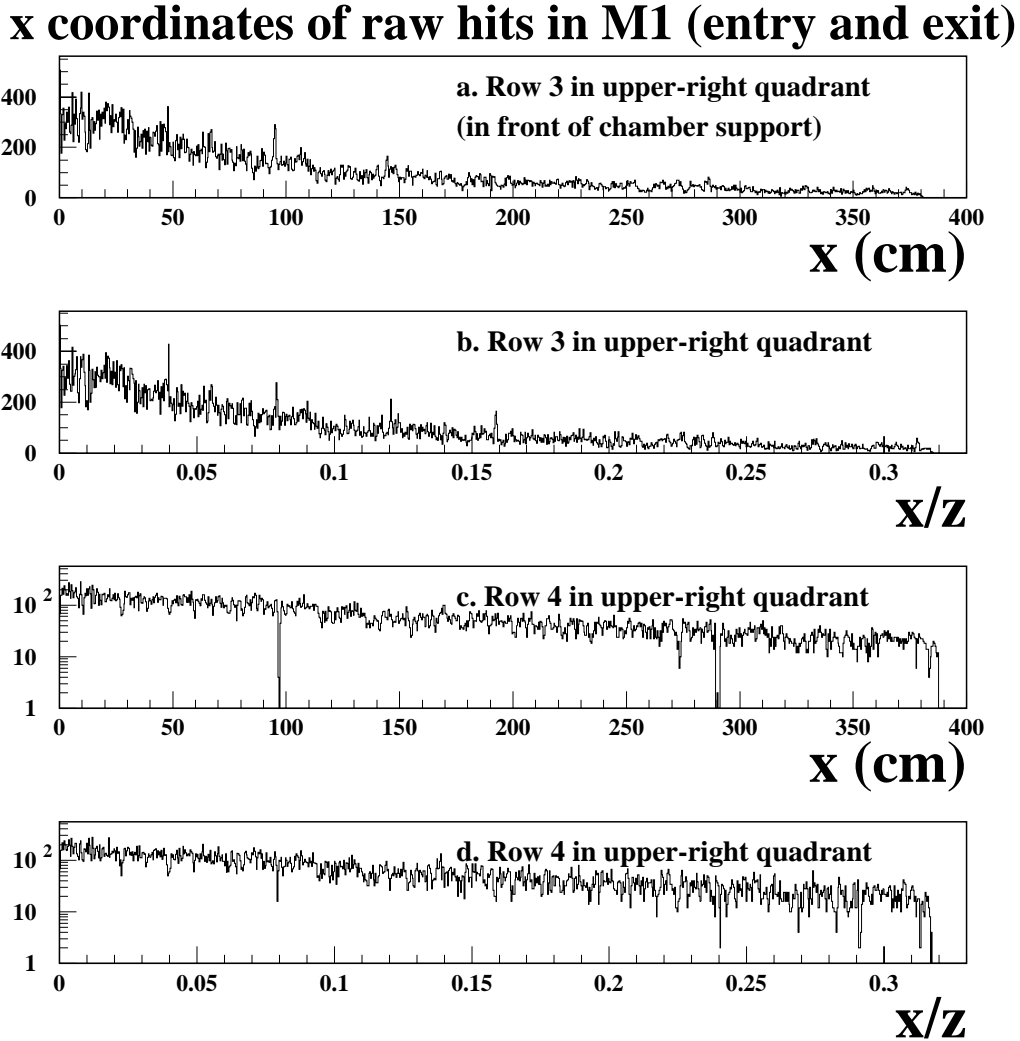


Figure 6: Distributions of track entry and exit points (hits) in station M1. The first plot shows the  $x$  distribution relative to chamber row 3 (in front of the chamber support) in the upper-left quadrant. The second plot shows the  $x/z$  distribution relative to the same chambers. The third plot shows the  $x$  distribution relative to chamber row 4 (behind chamber support), and the fourth plot shows the corresponding  $x/z$  distribution. The interpretation of the plots is discussed in the text.

Fig. 6a. shows the distribution of  $x$  coordinates for track entry and exit points in chamber row 3 of station M1. The chambers of row 3 are all in front of the chamber support, with the centres of adjacent chambers separated by 67.0 mm in  $z$ . Enhancements of the hit rate are evident at chamber boundaries, and are a consequence of the chamber overlap when looking

## y coordinates of raw hits in M1 (entry and exit)

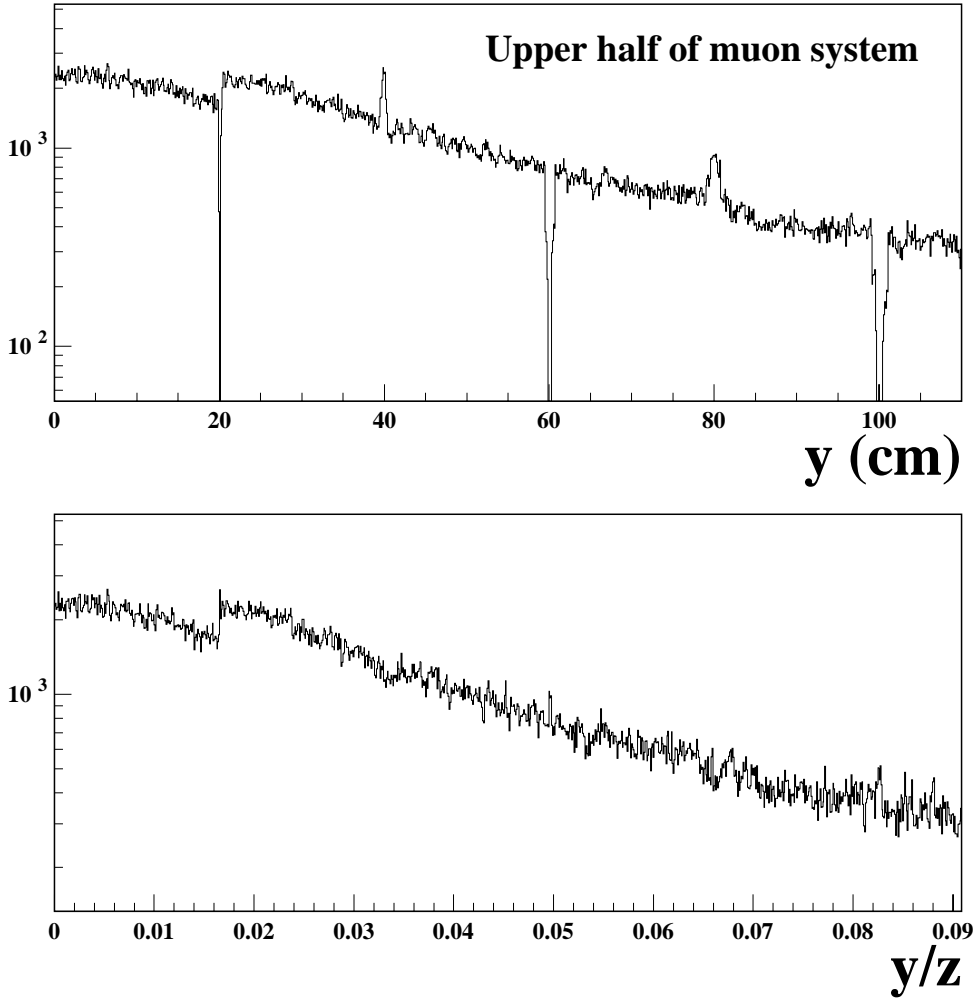


Figure 7: Distributions of track entry and exit points (hits) in the upper half of station M1. The upper plot shows the distribution of y coordinates and the lower plot shows the  $y/z$  distribution.

parallel to the beam pipe. Fig. 6b. shows the corresponding hit distribution as seen from the interaction point. The chamber overlaps are still visible, but enhancements in the hit rate are reduced.

Figs. 6c. and 6d. are similar to Figs. 6a. and 6b. but refer to the chambers of row 4. These chambers are behind the support, and there are holes between them in x when viewing parallel to the beam. The holes are less significant when looking from the interaction point, and for muons from the interaction region should not introduce any appreciable inefficiency.

Fig. 7 shows the distribution of y coordinates of track entry and exit points in the upper half of station M1. Enhancements and depletions in the hit rate are evident when looking parallel to the beam pipe (upper plot), but, as expected, disappear when looking from the interaction point (lower plot).

Fig. 8 shows the distributions in x-z and y-z of track entry and exit points in stations M1 and M4. Individual chambers are clearly identifiable. In station M4, the 4-gap MWPCs in regions R1 and R2 and the 2-gap RPCs in regions R3 and R4 are readily distinguished.

From the plots presented, we conclude that the software implementation of the muon-system geometry is correct, and that the chosen layout effectively covers the whole area of each station, without significant overlaps or holes as seen from the interaction point.

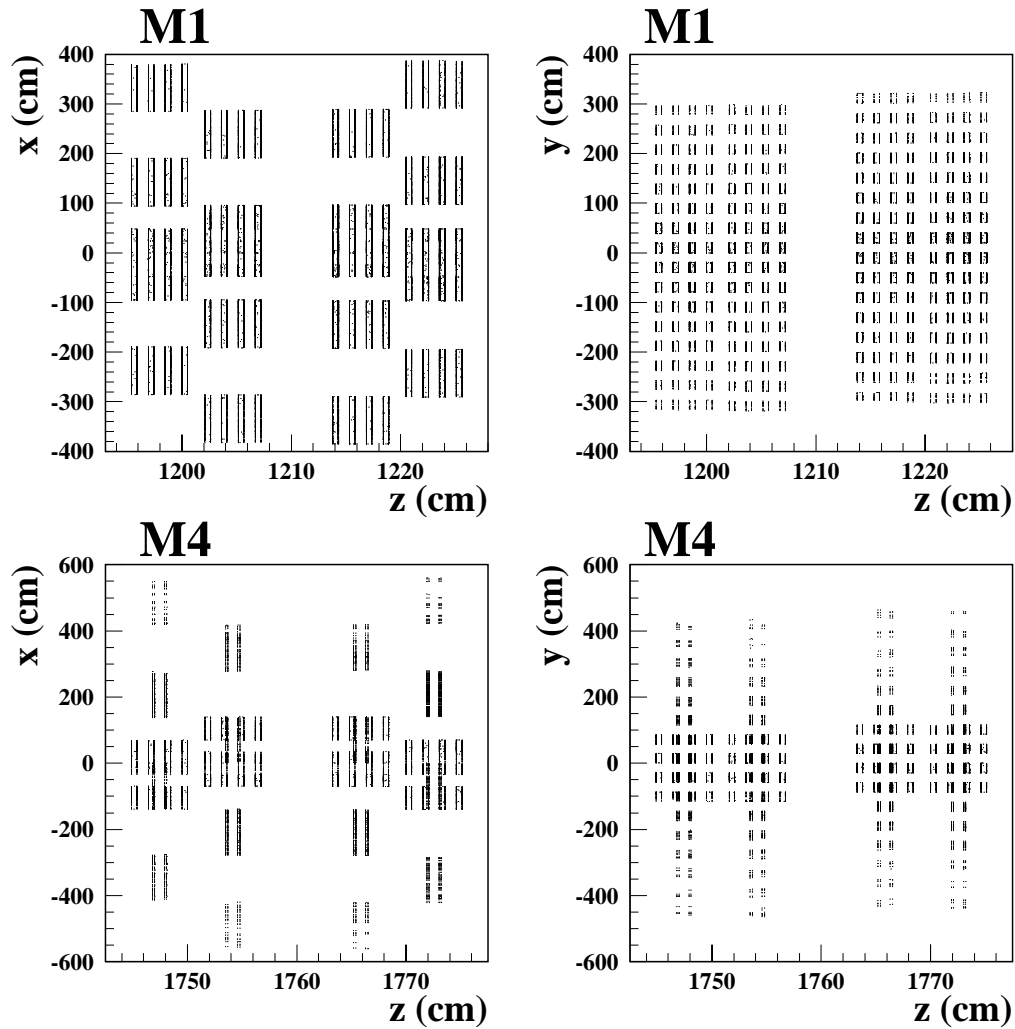


Figure 8: Distributions in x-z and y-z of track entry and exit points (hits) in stations M1 (upper) and M4 (lower)

## Acknowledgements

This work was supported by the Brazilian funding agency CNPq, and by Fundação José Bonifácio, UFRJ.

## References

- [1] P. Colrain and B. Schmidt, *Optimization of muon system layout*, LHCb 2000-016 Muon (2000).
- [2] B. Schmidt, *LHCb muon system by numbers*, LHCb 2000-089 Muon (2000).
- [3] A. Lai *et al.*, *Muon front-end architecture*, LHCb 2000-017 Muon (2000).
- [4] GEANT Detector Description and Simulation Tool, CERN Program Library Long Writeup W5013 (1993).